

Role of the electro-thermo-mechanical multiple coupling on the operation of RF microswitch

Original

Role of the electro-thermo-mechanical multiple coupling on the operation of RF microswitch / Brusa, Eugenio; Munteanu, M. G. h.. - In: MICROSYSTEM TECHNOLOGIES. - ISSN 0946-7076. - STAMPA. - 18:(2012), pp. 983-995.
[10.1007/s00542-012-1426-z]

Availability:

This version is available at: 11583/2475181 since:

Publisher:

Springer

Published

DOI:10.1007/s00542-012-1426-z

Terms of use:

This article is made available under terms and conditions as specified in the corresponding bibliographic description in the repository

Publisher copyright

(Article begins on next page)

Role of the electro-thermo-mechanical multiple coupling on the operation of RF-microswitch

Eugenio Brusa · Mircea Gheorghe Munteanu

Abstract A phenomenological approach is proposed to identify some effects occurring within the structure of the microswitch conceived for radio frequency application. This microsystem is operated via a nonlinear electromechanical action imposed by the applied voltage. Unfortunately, it can be affected by residual stress, due to the microfabrication process, therefore axial and flexural behaviors are strongly coupled. This coupling increases the actuation voltage required to achieve the so-called “pull-in” condition. Moreover, temperature may strongly affect strain and stress distributions, respectively. Environmental temperature, internal dissipation of material, thermo-elastic and Joule effects play different roles on the microswitch flexural displacement. Sometimes buckling phenomenon evenly occurs. Literature show that all those issues make difficult an effective computation of “pull-in” and “pull-out” voltages or evenly distinguishing the origin of some failures detected in operation. Analysis, numerical methods and experiments are applied to an industrial test case to investigate step by step the RF-microswitch operation. Multiple electro-thermo-mechanical coupling is first modeled to have a preliminary and comprehensive description of the microswitch behavior and of its reliability. “Pull-in” and “pull-out” tests are then

performed to validate the proposed models and to find suitable criteria to design the RF-MEMS.

1 Introduction

Prediction of reliability of the microswitch device used in radio frequency applications looks rather difficult because of a number of coupling effects superimposed in its operation. Literature clearly state that damage mechanisms are basically depending on the plastic behavior of material (Rebeiz 2002), static rupture (Tabata 2008), fatigue (Espinosa 2006) and thermal fatigue (Nieminen 2004, Goldsmith 2005), fracture and creep (Rezvanian 2008), wear and electric failures (Reid 2003). Nevertheless, operation of the RF-microswitch may lead evenly to a collapse due to buckling (Shamshirsaz 2008) or to a dynamic resonance (Brusa and Munteanu 2006a; Brusa 2006c). Mechanical design of the RF-microswitch consequently requires an extensive experimental identification of its static and dynamic behaviors, respectively, to prevent some critical conditions in operation (Sadek et al. 2009). Strength of material has to be tested as it looks at microscale and after the microfabrication process (Baek et al. 2005). Among the relevant tests performed on the microswitch “pull-in” and “pull-out” values of voltage are critical to identify the microsystem functionality. Pull-in voltage corresponds to the electromechanical action required to overcome the elastic restoring force in bending and to achieve the shortcircuit. Pull-out is related to the repulsive action required to the fixed electrode to switch off the RF-MEMS. A precise identification of those two conditions is crucial to effectively predict the actual response of the microswitch in operation and its life. Pull-in and pull-out phenomena are very seldom easily predicted, because they are affected by several phenomena occurring during the

E. Brusa (✉)

Department of Mechanical and Aerospace Engineering,
Politecnico di Torino, C.so Duca degli Abruzzi 24,
10129 Torino, Italy
e-mail: eugenio.brusa@polito.it
URL: <http://www.polito.it>

M. G. Munteanu

Department of Electrical, Management and Mechanical
Engineering, University of Udine, Via delle Scienze 208,
33100 Udine, Italy
e-mail: munteanu@uniud.it
URL: <http://www.uniud.it>

microswitch actuation. Up to now the intrinsic nonlinearity of the electromechanical coupling in static and dynamic behaviors was already deeply investigated and modeled by several authors, including those of this paper (Jing 2003; Reid 2003; Brusa et al. 2004; Ballestra et al. 2008; Bettini et al. 2008). Interaction between electromechanical actions and environmental fluid surrounding the MEMS was evenly analysed (Veijola et al. 2009). Only recently research activities were focused on the temperature role in microswitch functionality and reliability (Hasiang Pan 2002; Nieminen et al. 2004; Zhu and Espinosa 2004; Goldsmith 2005; Kang 2005; Rezvanian 2008; Bognar 2009; Yan 2009; Mahameed 2010; Saedivahdat 2010; Zamanian 2010). Unfortunately, conclusions and remarks are still in contrast each other. Only seldom multiple electro-thermo-mechanical coupling was completely investigated. Moreover, pre-liminary models and experiments performed, taking into account for the superposition of heating and electromechanical actuation, show different results and state discordant claims about the microswitch response. Dependence of pull-in and pull-out voltages, respectively, on the temperature condition is a key issue in those investigations. Some-times values of pull-in voltage look increased, in presence of a heating effect (Jing 2003). Some particular conditions motivate a poor dependence upon temperature, which was monitored at least at the very beginning of the heating process (Yan 2004). Several authors are prone to consider a decreased pull-in voltage for higher values of temperature (Zhu 2004; Goldsmith 2005; Zamanian 2010). Some uncertainties were found even in pull-out prediction. A larger contact between microstructure and fixed electrode due to thermal elongation motivates a stronger constraining action of the fixed electrode, according to some references, and a delayed pull-out (Rezvanian 2008). Spontaneous pull-out, even in case of actuated microswitch, was evenly monitored (Lin 2000). Sometimes a sudden pull-out is then followed by an unforeseen rupture (Subhadeep 2006). Since references include numerical and experimental results, which look basically consistent, authors were motivated in investigating the origin of the differences detected in those tests and finding some basic criteria suitable for the RF-microswitch design.

2 Methodologies

Coupled electro-thermo-mechanical behavior of an industrial prototype of RF-microswitch was first performed by resorting to a preliminary numerical investigation based on the Finite Element Method (Brusa and Munteanu 2006b). A reference geometry of microbridge electrostatically actuated was analysed through the ANSYS® code. A plane model of clamped-clamped microbeam was discretized by

160 structural shell elements coupled to the electric field by means of 40 so-called transducer elements, available into the commercial code. These elements allow computing the electromechanical forces exerted through the airgap by the fixed electrode on the nodes of the microstructure, by avoiding the discretization of the gap volume. They convert energy from the electric domain to the structural one and viceversa. Moreover, a simultaneous analysis of both the electromechanical and contact effects was performed.

Several geometries were investigated, although the numerical results here documented concern set of microbridges depicted in Fig. 1 and exhibiting the geometrical properties described in Table 1. It was demonstrated that main problems in modeling the so-called “out-of-plane” bending microbridges are related to the discretization of a narrow gap when a full integrated approach is applied (Brusa and Munteanu 2006a). In this case transducer elements allow a fairly good prediction of microstructure contact with the fixed electrode and decrease the computational time, usually spent to remesh the airgap, each time step of the nonlinear solution (Brusa and Munteanu 2006b). For all the above described samples airgap was measured and it was found very close to $3.0 \pm 0.5 \times 10^{-4} \mu\text{m}$. Microstructures were microfabricated by Fundation Bruno Kessler (FBK®) in Trento (Italy). Dimensions were measured even by means of the Zoom Surf 3D Fogale® profilometer according to procedures assessed in (Brusa 2010b; Soma 2010). Values reported in Table 1 include the equipment resolution on the wafer plane, being $0.3 \mu\text{m}$, while along the focal axis this value is $0.5 \times 10^{-4} \mu\text{m}$.

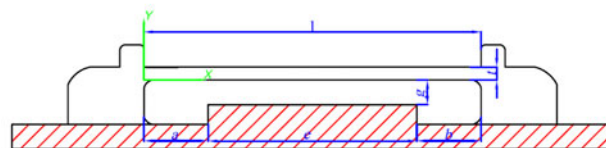
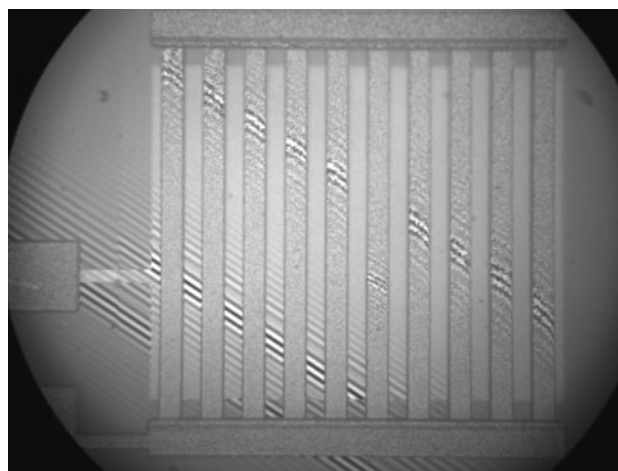


Fig. 1 Picture and sketch of the set RF-microswitches modeled and tested in this study

Table 1 Geometrical parameters and mechanical properties of tested microbridges

Units	MEMS 1	MEMS 2	MEMS 3	MEMS 4	MEMS 5	MEMS 6	MEMS 7	MEMS 8	MEMS 9	MEMS 10
Length [μm]	544.5 ± 0.3	545.6 ± 0.3	545.6 ± 0.3	547.9 ± 0.3	546.3 ± 0.3	544.8 ± 0.3	546.9 ± 0.3	545.7 ± 0.3	547.3 ± 0.3	546.6 ± 0.3
Width [μm]	34.9 ± 0.3	32.5 ± 0.3	34.4 ± 0.3	35.4 ± 0.3	33.5 ± 0.3	34.5 ± 0.3	33.9 ± 0.3	32.7 ± 0.3	35.0 ± 0.3	34.8 ± 0.3
Thickness [μm]	2.839 ± 0.5 $\times 10^{-4}$	2.932 ± 0.5 $\times 10^{-4}$	2.855 ± 0.5 $\times 10^{-4}$	2.936 ± 0.5 $\times 10^{-4}$	2.889 ± 0.5 $\times 10^{-4}$	2.901 ± 0.5 $\times 10^{-4}$	2.878 ± 0.5 $\times 10^{-4}$	2.920 ± 0.5 $\times 10^{-4}$	2.856 ± 0.5 $\times 10^{-4}$	2.854 ± 0.5 $\times 10^{-4}$

Those resolutions are compatible with a good prediction of the RF-MEMS functionality, since airgap is the most critical value for microbeam bending, because its cubic power appears into the expression of the electrostatic force (Brusa 2006a). The Zoom Surf 3D Fogale[®] was used to perform a preliminary characterization of the microswitch geometry, then to actuate the microsystem up to pull-in voltage. It analyses areas from $100 \times 100 \mu\text{m}^2$ to $2 \times 2 \text{mm}^2$. Optical magnification $20\times$ was used to achieve resolutions above mentioned. Maximum displacements up to $400 \mu\text{m}$ can be measured, while power electronics can provide up to 200V , up to a frequency of 2MHz . To increase the environmental temperature each microswitch was mounted on a Peltier cell Fogale[®], which assures a uniform heating around the microsystem, stable after few seconds, with a precision of 0.1°C about the required temperature value. Temperature was measured by a PT100 thermal sensor, connected to a closed-loop control acting on the Peltier cell (Fig. 2).

Microfabrication procedure followed patented procedure ‘‘RF Switch (RFS) Surface Micromachining’’, fully described in (Margesin 2003; Subhadeep et al. 2006). Material is Gold, exhibiting a good electric conduction with a reduced sensitivity to wear and corrosion. Material

**Fig. 2** Experimental set-up with the Peltier Cell Fogale[®] and the Zoom Surf 3D Fogale[®]

properties certified by the microfabricator are Young modulus, $E = 98.5$ GPa, density, $\rho = 19.32 \cdot 10^{-15}$ kg/ μm^3 , Poisson coefficient, $\nu = 0.42$ and thermal expansion coefficient, $\alpha = 14.3 \cdot 10^{-6}$ °C $^{-1}$. Strength of material was fully characterized in (Soma` 2009).

3 Thermo-mechanical coupling in absence of electro-mechanical actuation

3.1 Preliminary remarks

A sketch of microswitch is proposed in Fig. 1. Structure is a very thin and deformable gold strip, clamped at both ends by massive anchors. Fixed electrode is massive and fills only a part of the volume under the microbridge. Its dimensions define the contact area on which the microbeam is bent when it is actuated. Airgap looks fairly small if it is compared to the microbeam length, while microbeam width and thick-ness are evenly smaller than the microbridge length. These properties suggest that anchors should be stiffer than microbeam, there is a stress concentration around the clamps and gap is quite narrow. Dimensions of fixed elec-trode provide a good contact surface, after pull-in occurring. Other examples in the literature show different aspect ratios among the relevant dimensions of the microswitch. Larger gaps may allow larger displacements and consequently a stronger nonlinear structural behaviour of microbeam, but meshing in the dielectric region looks easier. Nevertheless, it is worthy noticing that double clamps may cause a non-linear structural behaviour, even in presence of small flex-ural displacement. Geometrical nonlinearity associated to the electromechanical nonlinear coupling (Collenz et al. 2004) requires the implementation of some approaches developed by the authors based on a sequential solution (Brusa and Munteanu 2006a, b).

3.2 Residual stress and mechanical coupling

Microbridge is usually referred to as statically indeterminate structure because clamps inhibit a number of degrees of freedom larger than six, associated to the beam rigid body seen as a free solid in space (Timoshenko 1961). This state motivates the occurring of residual stress after microfabrication. Differences in the thermal expansion coefficients of gold and chrome, respectively used in the RF-MEMS process cause a residual strain distribution within the RF-MEMS after removal of chrome sacrificial layers. In microcantilever this effect is evident, because its free end is displaced from line axis and beam shows a curvature (Margesin et al. 2003). Residual strain is easily identified because curvature is first measured by a profiling system, then microbeam models allow computing the

amount of average strain present. When both ends are clamped, microbeam rotation is inhibited and residual strain is converted into an initial amount of stress, stretching the RF-MEMS structure along the beamline axis, described by coordinate x :

$$\sigma_{xx} = E \Delta\alpha \Delta T. \quad (1)$$

Being E the Young modulus and ν the Poisson coefficient of gold, respectively, while $\Delta\alpha$ and ΔT describe differences between thermal expansion coefficients and temperatures of gold and of substrate material. Residual stress is usually tensile, therefore microswitch geometry looks like unloaded. Unfortunately, this residual stress induces a mechanical coupling between the axial and flexural behaviours, respectively, by making stiffer the microbeam. Axial load increases the restoring action applied by the microsystem when it is bent, thus increasing the pull-in voltage. Flexural displacement, w , axial displacement, u , and axial loading, N , are nonlinearly coupled as follows:

$$N = EA \left[\frac{\partial u}{\partial x} + \frac{1}{2} \left(\frac{\partial w}{\partial x} \right)^2 \right]. \quad (2)$$

Microbeam axial stiffness is described by product EA , where A is the area of the beam cross section. Mechanical coupling is very well known and is usually taken into account in modelling (Lin 2000; Zhu 2004; Goldsmith 2005; Espinosa 2006), with few exceptions (Jing 2003). Samples described in Table 1 did show an increased value of pull-in voltage, even at their first actuation, if compared to the values simply computed according to some classical references (Rebeiz 2002). Provided that geometrical dimensions were precisely measured, this result could be related either to an existing axial loading, like in case of tensile residual stress, or to a imprecise measurement of elastic properties of gold, after microfabrication. Several microcantilevers microfabricated on the same wafer where microswitches were processed, allowed verifying and measuring the material elastic properties and detecting their first resonance frequency and pull-in voltage, as in (Espinosa et al. 2006; Ballestra et al. 2008). Actually resonance frequency and pull-in voltage are related to the elastic properties of material, therefore both those inputs led to verify the Young modulus of gold certified by the microfabricator, within a tolerance of few percents. Small differences among the samples did not justify the large mismatch of values between the actual pull-in voltage, about 70 V, and its numerical prediction of 35 V. Residual stress could be identified on samples by means of a dynamic test, based on an experimental detection of the first resonance frequency. Those experiments demonstrated that at least a residual stress of about 25–30 MPa could motivate the pull-in voltage measured. It is worthy noticing that temperature

increase may significantly change both the elastic properties of material and the residual stress exhibited at room temperature. Although poly-Silicon materials exhibit an appreciable sensitivity of thermal expansion coefficient and Young modulus on temperature, which becomes strongly nonlinear above a temperature threshold, in case of gold this dependence is less effective, according to experiments described by Collard (1991). Between 23° and 120°C, gold used for microfabrication looks exhibiting a linear variation of the Young modulus with the increasing temperature and its value decreases at 120°C of 2% of the magnitude measured at room temperature. This change is comparable to the error of direct measurement performed by means of the above mentioned procedures. Even residual stress is not stable over time, especially when structure is simultaneously excited by mechanical and thermal loading. Temperature may induce a relaxation effect on the residual stress (Epp 2011; Medvedeva et al. 2011). Therefore after few thermal loading cycles residual stress effect may look vanishing as in (Margesin et al. 2003; Mulloni et al. 2010). This fact may motivate even significant differences in pull-in and pull-out values after a defined period. Nevertheless, it looks very difficult predicting this sort of decay rate of residual stress action.

3.3 Heating of electromechanically uncoupled microsystem

When heating occurs before that the microswitch is actuated thermal effects and residual stress affect simultaneously the pull-in voltage, so as static and dynamic responses of microbridge are significantly changed (Zamanian 2010). If temperature increases all around the RF-MEMS, a uniform dilatation of the microbeam is excited, but is inhibited by the clamps. Therefore a compressive load is applied to the microstructure. Its influence on pull-in is just opposite to the effect of tensile residual stress. Theoretically if the original shape of the beam is ideally perfect and load is perfectly aligned with its line axis, compressive load does not induce any bending on the microsystem, as well as some authors claim even recently (Palego 2009; Saeedivahdat 2010). Actually, in real microsystems behaviour is different. For instance, tested case for a temperature increasing from 25 to 70°C shows the deformed shape depicted in Fig. 3. It is upwards, with respect of the fixed electrode. This result is quite common (Lin and Chiao 2000; Jensen 2003), although sometimes deflection occurs even towards the shortcircuit as in Kang et al. (2005).

Those differences depend on some boundary conditions. Deformed shape may be motivated by a non symmetric layout of anchors, which can exhibit a slight difference in the rotation allowed when flexural displacement of microbeam is respectively upwards or downwards. Small

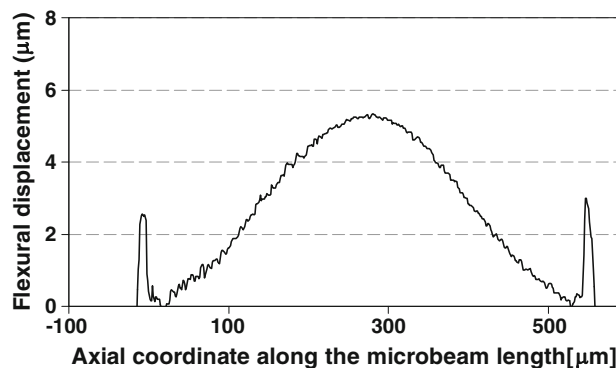


Fig. 3 Microswitch profile detected by the Zoom Surf 3D Fogale® on a tested sample in presence of heating from 25 to 70°C

eccentricities of the line axis or even a slight curvature of microbridge may lead to a preferable direction for bending. Residual stress gradient across the microswitch thickness as well as a temperature difference between the upper and lower surfaces may induce the monitored deformation. In addition has to be considered that microstructure slenderness may allow the buckling phenomenon under compression, if the axial load applied overcomes the critical load of elastic instability (Timoshenko 1961). All these effects sometimes superimpose and the final result appreciated on the microsystem response is a sort of compromise among them. Numerical investigations performed by means of the Finite Element Method and some preliminary experiments allowed describing this superposition in the tested cases and distinguishing their separate roles on the microswitch operation, on each step of either electromechanical or thermal loading. A first set of numerical results demonstrates that even in case of non symmetric layout of anchors consequences upon the maximum flexural displacement of microbridge is limited, although this influence is increased as shorter is the microbridge. A preliminary studied was developed in (Brusa and Munteanu 2011). It was found out that difference in flexural displacement of microbeam, when deflection occurs upwards or downwards, respectively, is poorly appreciable for higher values of microbeam length, for given values of gap and thickness. Even in case of shorter microbeam this difference consists of few percents of the microbridge length. Therefore this item looks insufficient to motivate a considerable tendency of the microstructure to bend along a preferable direction. Only in case of buckling, even this small difference may induce the collapse in a defined direction. Significantly larger effects are detected if residual stress is present on the microswitch after the microfabrication process (Margesin et al. 2003). Therefore evaluating the amount of residual stress on the microstructure is a key action of the microtechnological characterization of MEMS (Tabata et al. 2008; Szabo et al.

2009). Modelling and measuring this stress distribution along the microbeam thickness is practically impossible, but an average value can be approximately computed by following the identification procedure based either on pull-in measurement or frequency shift detection (Soma` et al. 2010). Definitely simpler is prediction of the mechanical coupling between flexural and axial loading, when temperature gradients are applied across the microbeam section. Stress along line axis, σ_{xx} , is computed as follows:

$$\sigma_{xx} = -\alpha E \frac{2\Delta T}{h} y. \quad (3)$$

Being ΔT the temperature difference between the upper and lower surfaces, y the direction along the beam thickness, called h . Higher values of temperature on the lower surface induce a compressive loading, while the upper surface is stretched. In the tested case an average residual stress of 25–30 MPa was detected, as it was above mentioned, in addition a uniform heating of the microswitch simultaneously induced a compressive loading up to the critical value at which buckling occurred. Direction of flexural displacement was motivated by a slightly lower rotational inertia of microbeam in the out-of-plane bending, with respect of the wafer layer combined to a small difference of temperature between the upper and lower surfaces, respectively. The latter was motivated by the location of the Peltier cell under the RF-MEMS frame. Microstructure slenderness allowed the buckling occurring.

3.4 Thermomechanical buckling and spontaneous pull-in

To predict the buckling phenomenon due to the temperature increase a simple analytical model was implemented and updated to the current case (Gupta 2008). If microswitch is simply heated, without any electromechanical action, buckling occurs at the so-called critical load, P_{cr} , if critical temperature T^* is reached. This threshold can be computed by equalling the critical and thermal loads, respectively as follows:

$$P_{cr} = \frac{4\pi^2 EI}{L^2}; \quad P_{term} = \alpha(T^* - T_0)EA; \\ T^* = T_0 + \frac{4\pi^2 I}{\alpha A L^2} = T_0 + \frac{1}{3\alpha} \left(\frac{\pi h}{L} \right)^2 \quad (4)$$

where symbols meaning is microbeam length, L , second order moment of area (transversal and minimum) of cross section, I , initial or reference temperature, T_0 , threshold temperature, T^* , cross section area, A , thermal expansion coefficient of gold, α . Test case has rectangular cross section with dimensions b and h . Dimensions described in Table 1, allow computing preliminarily the critical load, $P_{cr} = 1,020 \mu\text{N}$, as well as the threshold temperature, $T^* = 30^\circ\text{C}$. Assuming that the operational range for gold

RF-MEMS approximately rises up to 70–120°C, this threshold looks included. Therefore post-buckling behaviour has to be considered and predicted. An effective approach was developed by Gupta et al. (2008). Rayleigh–Ritz method was there used to solve the proposed elastic problem. Boundary conditions were applied by imposing effects of constraints, then flexural displacement was computed at the middle-span section, $x = L/2$, by identifying the corresponding thermal loading required to induce the collapse. Lateral displacement of microbeam, w , is there assumed to be:

$$w(x) = \frac{a}{2} \left(1 - \cos \frac{2\pi x}{L} \right). \quad (5)$$

Which allows computing the total load applied, P_{TOT} , and the axial displacement, u . In case of clamped–clamped microbeam following expressions can be found:

$$P_{ad} = \frac{\pi^2 a^2 EI}{4L^2 r^2}; \quad u(x) = \frac{a^2 \pi}{16L} \sin \frac{4\pi x}{L}. \quad (6)$$

Being coefficient a the amplitude of function $w(x)$ in Eq. (5), which describes the flexural displacement of middle-span cross section, while $r = (I/A)^{0.5}$. For given P_{ad} threshold temperature T^* is easily computed. Practically, if load is first computed for increasing values of a , i.e. of flexural displacement, Eq. (6) allows identifying each corresponding temperature, T , as follows:

$$T(a) = T_0 + \frac{1}{3\alpha} \left(\frac{\pi h}{L} \right)^2 \left(1 + \frac{12a^2}{16h^2} \right) \\ = T_0 + \Delta T^* + \frac{\pi^2 a^2}{4\alpha L^2}. \quad (7)$$

In Eq. (7) three components can be appreciated. Reference temperature, T_0 , corresponds to the unloaded and stand-alone configuration. Temperature difference ΔT^* is required to increase the microswitch deflection up to the buckling threshold, corresponding to temperature T^* . Last contribution gives the additional deflection caused by the post-buckling loading as a function of material, geometry and load parameters. Moreover, if residual tensile stress σ_0 is considered, the temperature characteristic law in post-buckling regime becomes:

$$T(a) = T_0 + \Delta T^* + \frac{\pi^2 a^2}{4\alpha L^2} + \frac{\sigma_0}{E\alpha}. \quad (8)$$

If microbeam is deflected by buckling phenomenon before that electromechanical actuation is applied, its response significantly changes as well as pull-in voltage. Buckling does not automatically corresponds to yielding of material. Very often, when loads are removed, restoring actions bring the microstructure to the original shape, without any plastic strain. This principle is widely used in deployable structures (Motro 2010). Few cases of failed

microbridges prone to spontaneous pull-in after micro-fabrication process were found in the literature and associated to the temperature increasing (Rocha et al. 2003). Actually, in those tests thermal effects, residual stress and additional process consequences induced downwards bending of microbridge instead of upwards displacement, even for a small increment of temperature. Deflection was sufficient to bring deformed shape in contact with the fixed electrode and to an accidental shortcircuit. This condition is found when pull-in looks to be surprisingly null, because microstructure is actuated when it is already in wide contact with the fixed electrode (Jing 2003). Trends above described in buckling could be numerically predicted in the test cases considered for this analysis by assuming a very small initial elastic eccentricity of the middle span cross section, either upwards and downwards respectively. As Fig. 4 shows a small increment of temperature could induce in the first case above mentioned a deformed shape upwards, up to the buckled shape described in Fig. 3, occurred at a temperature corresponding to T^* . When deformation is downwards, as in Fig. 4a, a spontaneous pull-in can be easily achieved, if temperature is sufficiently increased. In this case if temperature continuously grows up a larger contact on the fixed electrode surface is first found, but above a secondary critical load structure may even snap up, reaching the deformed shape described in Fig. 4b.

3.5 Critical issues of the stand-alone configuration

This preliminary analysis allows summarizing some relevant remarks. Apparent undeformed shape of microbridge after microfabrication process does not necessarily correspond to an unloaded configuration, since residual stress may be present. It is usually tensile and may induce the micro-structure to bend either upwards or downwards, when temperature increases. A sort of stiffening effect is perceived, since pull-in voltage increases. Nevertheless, residual stress effect is usually antagonist of thermal loading, which induces

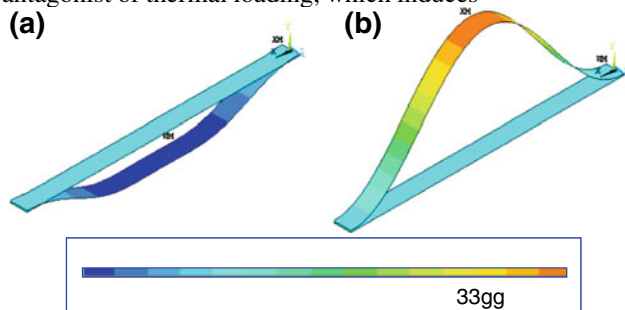


Fig. 4 Numerical investigations performed on the test case to predict the flexural displacement in case of increasing temperature up to buckling with **a** contact with electrode **b** free bending out-of-plane (displacement units are shown as a function of the initial gap, g , and magnified)

a compressive axial stress which tends to decrease the required action to reach the pull-in condition. Residual stress undergoes a relaxation phenomenon up to vanish after a defined time (Epp et al. 2011). Therefore short, mid-term and long-term experimental observations performed on the same microswitch in operation, documented in the literature, can be understandably different and even consistent. In presence of pure heating without electromechanical coupling, buckling phenomenon may lead to have large deformed shapes of the microbridge. This phenomenon occurs for instance within the temperature operational range of the tested sam-ples. If flexural displacement is downwards, shortcircuit is easily achieved and potentially microswitch failures occur at the very beginning of actuation. When displacement is upwards deformation may be larger, sometimes leading to reach a consistent bending stress, causing even yielding or rupture. Open question in the literature is whether buckling phenomenon increases or decreases pull-in and pull-out voltages, respectively. Superposition of several effects above mentioned give different results depending on the microsystem aspect ratios and dimensions, since each phenomenon may be potentially dominant upon the others.

4 Microswitch operation under electro-thermo-mechanical action

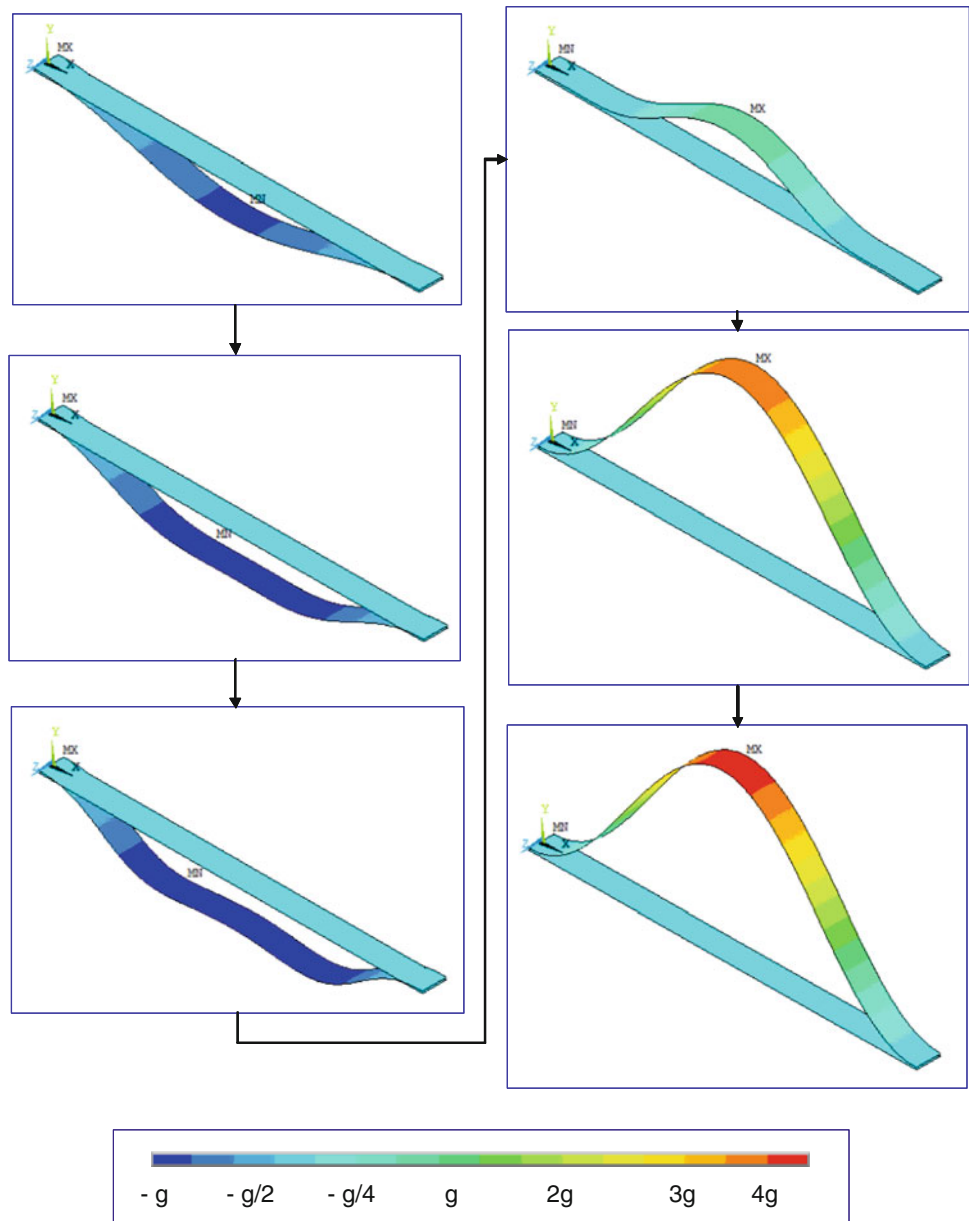
4.1 Buckling effect on the pull-in and pull-out phenomena

To complete the proposed analysis and to solve the last doubts above expressed, a complete nonlinear electro-thermo-mechanical model of microswitches described in Table 1 was developed in ANSYS[®]. Some typical sequential actuations over time were simulated. Results are shown for the average values of the samples design parameters. In particular inputs were set at $L = 540 \mu\text{m}$, $b = 34 \mu\text{m}$, $h = 3 \mu\text{m}$, $E = 98,500 \text{ MPa}$, $\nu = 0.42$, $\alpha = 14.3 \cdot 10^{-6} \text{ K}^{-1}$ and gap $g = 2.9 \mu\text{m}$. A sequence of thermal and electro-mechanical loading conditions was applied. Iterative and sequential approaches to solve the coupled problem were implemented according to (Brusa and Munteanu 2006a, 2006b; Ballestra et al. 2008; Bettini et al. 2008; Brusa et al. 2010b; Soma` et al. 2010). Among several numerical results obtained only the most impressive results will be herein proposed. In Fig. 5 loading sequence applied in the FEM model is described. Sample was initially heated up to $T = 30^\circ\text{C}$. Boundary conditions were applied to induce a preferable positive deflection towards the fixed electrode. Microbridge initially bent down, without shortcircuit. It was sufficient applying an actuation voltage of 15 V to reach then the contact between microswitch and fixed electrode, instead of 34 V corresponding to pull-in voltage in case of

undeformed configuration and null residual stress. All typical forces, associated to charges attraction and middle and low range interaction, were activated by contact (Brusa 2010a). In this configuration a pull-out voltage is usually required to help restoring force to switch off the microbeam. It was assumed that in presence of constant voltage temperature could increase because of shortcircuit. Actually Joule effect applies to the microswitch in contact with the fixed electrode, because of the current. In real actuation frequency is fairly high, actuation is dynamic and contact is closed for short periods of time. Nevertheless, an average heating effect is often measured like if microsystem were almost continuously heated, since conduction is not sufficiently fast to deliver the heat stored within the structure,

during the switching off (Lin and Chiao 2000). Model assumes that temperature gradually increases, up to a condition for which shape of microbeam is modified as Fig. 5 shows in first column down left. Temperature increasing induces a thermal elongation of the microbeam. Contact surface is first increased, thus helping the electromechanical action to keep the microswitch in contact. Nevertheless, when temperature reached a secondary critical value for buckling, suddenly the microstructure snapped up so fast that a large flexural displacement was achieved (Fig. 5, column right). This investigation shows that spontaneous pull-out may even occur, as some reference claims (Zhu and Espinosa 2004). Temperature increment of $\Delta T = 90^\circ\text{C}$ was required to reach this secondary buckling in simulation.

Fig. 5 FEM simulation showing the primary and secondary buckling phenomena applied to the microswitch under electro-thermo-mechanical loading



4.2 Stress prediction

A preliminary stress computation was performed for the simulated sequence of loading previously analysed. In all the deformed configurations of the microswitch typically two behaviours were excited. Bending occurs because of the axial to flexural coupling and to the electromechanical action, associated to the contact activated when pull-in is achieved. As usual in bending one surface of microbeam is mainly under tensile stress, while the opposite one is compressed. FEM model indicates that at first buckling, maximum tensile stress of 17 MPa is applied to the upper surface, while lower face is loaded by a compressive stress of 36 MPa. At pull-in tensile stress achieves 70 MPa and compressive stress is about 80 MPa. Contact mechanics significantly increases the stress level at the interface between microbridge and fixed electrode. In particular, close to the edges of fixed electrode, on the upper surface a large compression is appreciated and values are about 130 MPa, while on lower surface concentration is close to the clamps.

For gold this value overcomes the strength of material, of 120 MPa, although it applies to traction (Soma` 2009). After the second buckling stress level increases more. Fig. 6 summarizes the flexural displacement of the middle cross section and the stress variations for few cross sections of the microswitch as a function of time. Stress distribution changes significantly during the microswitch loading sequence and stress concentrations are present not only at the constraints or in the middle but also where electrode edges are located. They actually play the role of additional supports during the contact between the two bodies. Contact induces a significant compressive stress and excites the secondary buckling. Loading sequence was obviously idealized and only partially reproduces the microswitch operation. Nevertheless, even in case of different sequence over time, it includes at least some critical steps and deformed shapes to be considered in design. Moreover it looks explaining some interesting results found and documented in the literature. Residual stress was here neglected, but its role can be easily appreciated in the experimental results herein described.

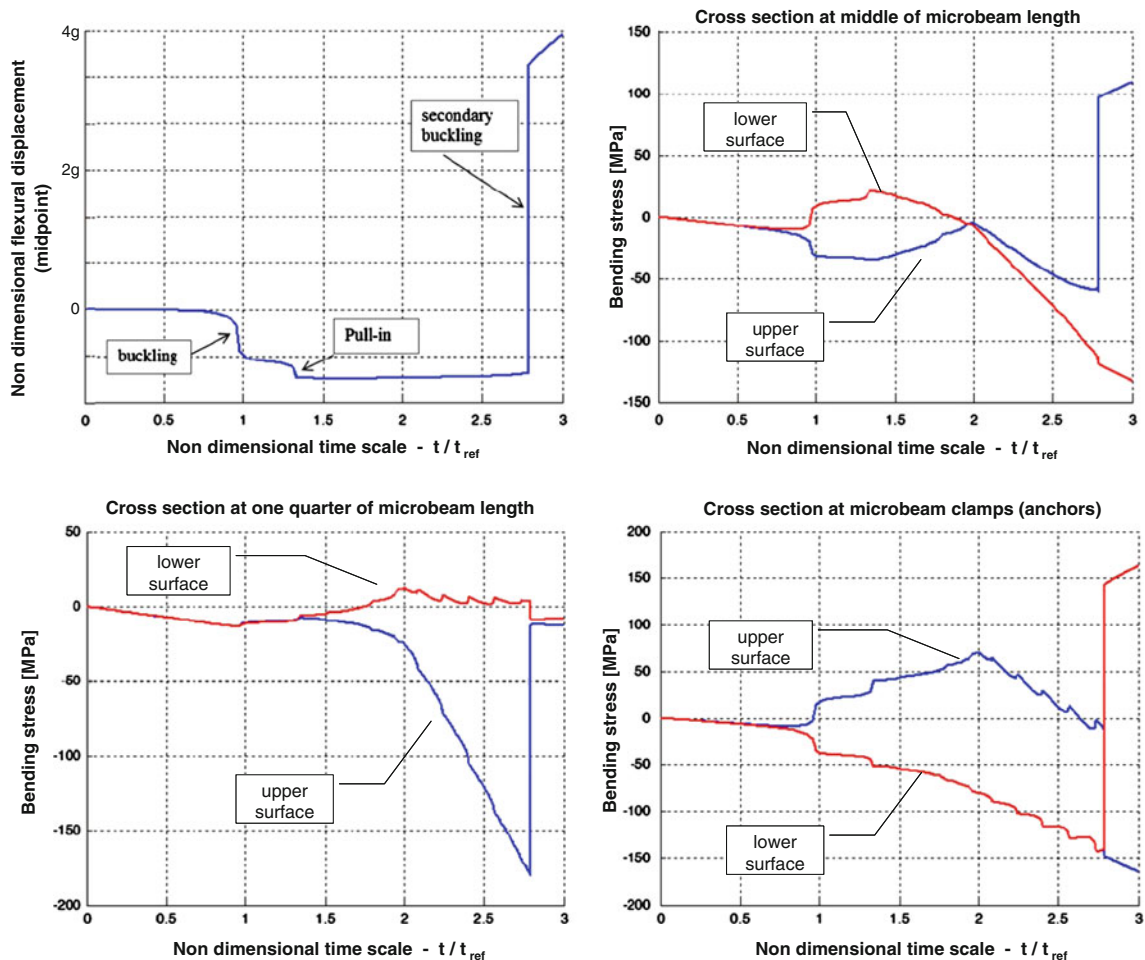


Fig. 6 Stress analysis plotted as a function of the non dimensional simulation time

4.3 Preliminary experiments

Tests were performed on prototypes by means of the Zoom Surf 3D Fogale[®] and Peltier Cell Fogale[®]. All samples described by Table 1 were tested. Every microsystem was observed several times during repeated loading cycles. In this preliminary activity two sessions were performed. In a first step only the thermo-mechanical coupling and buckling phenomenon were observed. Then a second session was aimed at studying pull-in and pull-out voltage in presence of electromechanical action at different values of temperatures. Loads were applied slowly and dynamic behavior was not yet observed. Nevertheless, this preliminary investigation was useful to distinguish the role of relevant phenomena, although further tests have to be performed to predict the actual behavior at the operation frequency.

A first screening was performed by applying an increasing thermal loading imposed by a gradual heating of microswitch, from the room temperature up to a test temperature, followed by a slow cooling. Test temperature was set at 70°C to avoid initially the destruction of microsamples. As Fig. 7 shows no hysteresis occurs when the heating and cooling loop is followed during the experimental test. Strain remains elastic and no effective damage occurs and actuation looks reversible, at least for this initial loading condition.

All the microsamples were tested by following this preliminary loading cycle based on a gradual heating followed by a slow cooling. Results are compared in Fig. 8. Buckling clearly occurs at a defined temperature, when flexural displacement suddenly increases and microbeam exhibits a large deformation upwards. Post-buckling behaviour is correctly predicted by the analytical model described in Eq. (4), Eq. (7) and Eq. (8). Heating induces a first small flexural displacement of microbeam cross section, up to the critical temperature T^* at which instability occurs. Above this temperature behaviour a postbuckling behaviour is considered, i.e. a geometrical nonlinear analysis is performed (Brusa 2010a). Agreement between model and experiments is good. Small dimensional differences in microsamples, described in Table 1, actually do not change significantly the mechanical response to heating up to buckling. Above the instability threshold some differences are appreciated. Nevertheless, this model, which implements the average values of design parameters, is suitable to predict, at least approximately the actual behaviour of the microswitch set. It is remarked that critical temperature for buckling is fairly higher than the value previously computed. This effect is due to the residual tensile stress induced by microfabrication process. Eq. (8) allows computing the corrected value of T^* corresponding to 30 MPa, identified by dynamic tests. In presence of

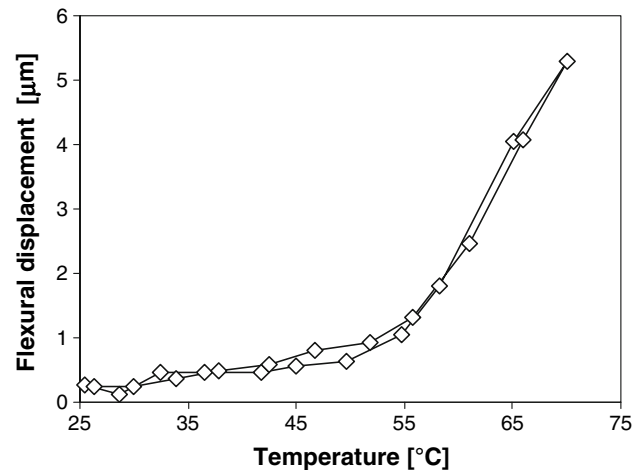


Fig. 7 Flexural displacement measured by the Zoom Surf 3D Fogale[®] in a complete heating-cooling loop during a preliminary experiment to investigate the thermo-mechanical coupling

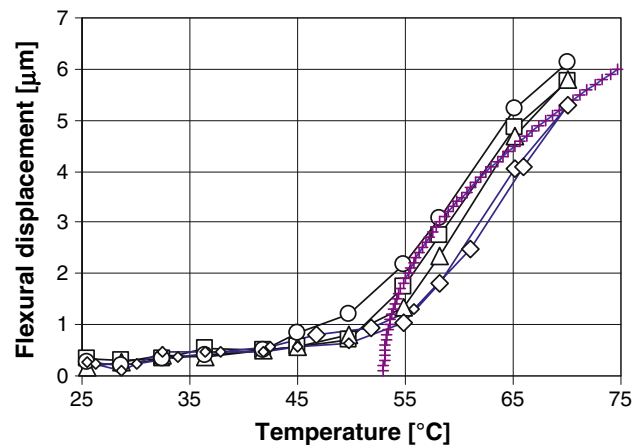


Fig. 8 Flexural displacement measured by the Zoom Surf 3D Fogale[®] and post buckling model validation

residual stress new value is about 53°C and fits the experimental evidence of Fig. 8. Moreover, it can be remarked that an inverse procedure could be even used to identify the residual stress stored by the microswitch during the microfabrication process, by detecting critical temperature T^* .

4.4 Electro-thermo-mechanical coupling

A loading condition more close to the actual operating conditions was finally tested. In this case play a significant role residual stress, heating and electromechanical actuation as well as buckling. A first result is appreciated in Fig. 9.

At room temperature microsample 1 shows a higher pull-in voltage than value computed without residual stress. As Fig. 9 shows pull-in voltage is up to 70 V. Tensile

action makes stiffer the microbeam because of the axial to flexural coupling. At higher temperature, i.e. 45°C, still lower than the instability threshold for buckling, pull-in voltage decreases to 53°C. Initial position looks negative because higher temperature induces an upwards deformation, which is antagonist with respect of fixed electrode and pull-in, being assumed to be positive. Compression caused by temperature reduces the apparent stiffness of microbeam. Since test temperature is still lower than buckling threshold, the restoring force is decreased while airgap is still sufficiently small to make the electromechanical force very effective. Pull-in is consequently quite easily obtained. This result fits experience documented by several authors (Rocha et al. 2003; Zhu 2004; Palego et al. 2009). When temperature overcomes the threshold required for buckling, deformed shape becomes similar to the last case depicted in Fig. 5. Pull-in voltage seems to be larger. Computation actually suggests that airgap is so large that electrostatic force is far less effective. Numerical prediction defines a higher pull-in voltage at which this condition is ideally achieved, but in practice, when microsample 1 was tested at 70°C pull-in was never achieved even in presence of a significant voltage. Fringing of electric field, large airgap and interaction with surrounding air, made in practice ineffective the electromechanical actuation when microswitch snap up was so large. This evidence motivates some statements, which are prone to consider pull-in voltage larger in case of electro-thermo-mechanical coupling and increasing temperature. A final open question was whether secondary buckling and spontaneous pull-out is real or a pure numerical prediction. To verify this item microsamples were kept in pull-in condition by imposing a constant voltage slightly larger than pull-in value, then

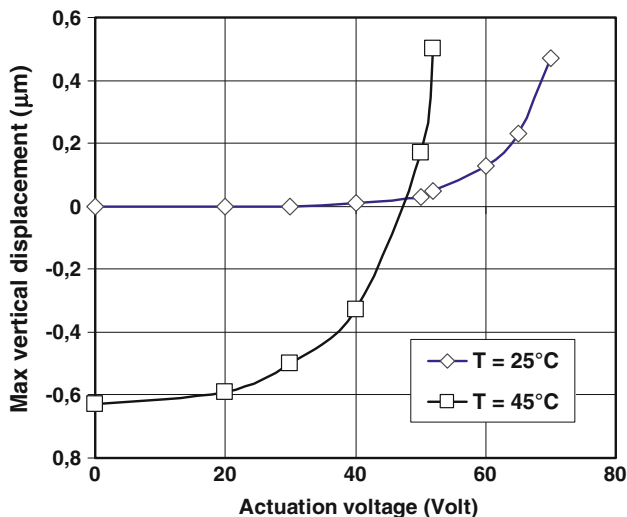


Fig. 9 Pull-in tests performed in presence of residual stress, at two different values of temperature

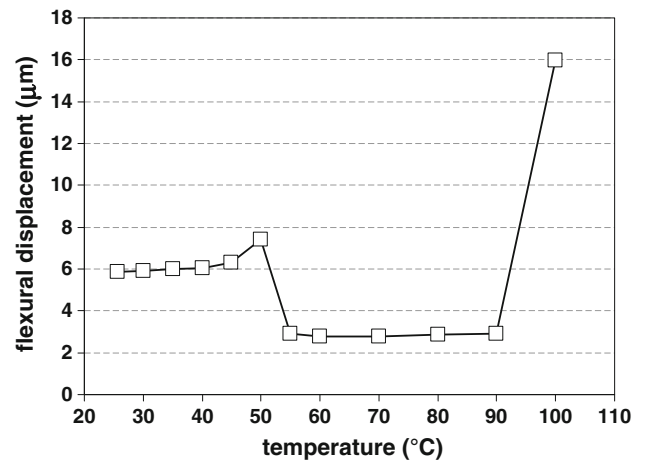


Fig. 10 Example of secondary buckling of the actuated microswitch occurring after pull-in when temperature increases

temperature was increased. As Fig. 10 in case of microsample 8 numerical prediction is somehow consistent with actual behaviour of microswitch. Pull-in is first achieved for 51 V, when contact remains active up to the threshold of the secondary buckling, occurring when temperature grows up to 90°C. Microbeam suddenly snaps up and air-gap is significantly larger than the nominal one, because microbeam elongation at that temperature is fairly large. Actually pull-in was never possible, after this collapse, even if voltage was significantly increased.

5 Conclusions

Microswitch operation is strongly affected by several phenomena simultaneously superimposed. In case of gold material their effects appear fairly evident. Residual stress, heating, buckling phenomenon and multiple coupling caused by the interaction between axial and flexural behaviours and electro-thermo-mechanical actions all concur to define the actual values of pull-in and pull-out voltage as well as the structural reliability of this RF-MEMS. A comprehensive analysis of all those aspects was performed. Numerical and experimental evidences demonstrated that pull-in and pull-out voltages may be significantly changed by all those influences. Compliance of massive anchors has to be evaluated case by case, although its role is usually marginal if compared to the other phenomena. Tensile residual stress significantly increases pull-in voltage, at least up to relaxation induced by a permanence at higher temperature or by several thermomechanical loading cycles. If buckling of microswitch occurs before the electromechanical actuation, microdevice can be either shortcircuited or pull-out from the fixed electrode. Temperature increasing induces a compressive action on the double clamped microsystem that decreases the

structural restoring force in pull-in, but can motivate a spontaneous pull-out, if secondary critical load for buckling is overcome, even when microswitch is kept in contact by voltage with fixed electrode. Buckled microstructures may show larger values of pull-in voltage if airgap is large. In some case stress induced is larger than the ultimate tensile stress of material. All those observations fit several evidences available in the literature, but some discordant. Actually a suitable interpretation of superposition of residual stress, temperature and buckling in addition to the electromechanical actuation allowed distinguishing the effects of all the above mentioned phenomena. This result can be carefully used to design new experimental set-ups aimed at studying the electro-thermo-mechanical reliability of microswitch as well as to optimize the layout of RF-MEMS based on this layout.

Acknowledgments Authors appreciate the fundamental contribution of Prof. Aurelio Somà and Dr. Giorgio De Pasquale in the experimental activity performed at the Laboratory of Design and Testing of Microsystems of Politecnico di Torino, Italy.

References

- Baek C, Kim Y, Ahn Y, Kim Y (2005) Measurement of the mechanical properties of electroplated gold thin films using micromachined beam structures. *Sens Actuators A* 117:17–27
- Ballestra A, Brusa E, Munteanu MG, Somà A (2008) Experimental characterization of electrostatically actuated inplane bending of microcantilevers. *Microsyst Technol* 14(7):909–918
- Bettini P, Brusa E, Munteanu MG, Specogna R, Trevisan F (2008) Static behaviour prediction of microelectrostatic actuators by discrete geometric approaches. *IEEE Trans Magnetics* 44(6):1606–1609
- Bognar G, Szucs Z, Szekely V, Rencz M (2009) Contactless thermal characterization of high temperature test chamber. *Microsyst Technol* 15:1279–1285
- Brusa E (2006) Dynamics of mechatronic systems at microscale in “Microsystem Mechanical Design”. Springer Verlag, CISM Lectures Series, pp 57–80
- Brusa E (2010) Design for reliability of micromechatronic structural system in micro electro mechanical systems, MEMS: technology, fabrication processes and applications. Nova Science Publisher Inc, Hauppauge
- Brusa E, Munteanu M (2006a) Validation of compact models of microcantilever actuators for RF-MEMS application. *Analog Integr Circuits Signal Process* 59:191–199
- Brusa E, Munteanu M (2006b) Coupled-field FEM nonlinear dynamics analysis of continuous microsystems by non incremental approach. *Analog Integr Circuits Signal Process* 48:7–14
- Brusa E, Munteanu M (2011) Effect of electro-thermo-mechanical coupling on the short-circuit in RF microswitch operation. In *Proceedings of SPIE Microtechnologies 2011*, 18–20 April 2011, Prague Czech Republic, Conf. “Smart Sensors, Actuator and MEMS V”, Vol 8066, ISSN 0277-786X, ISBN 9780819486554, pp 80660W1–80660W15
- Brusa E, De Bona F, Gugliotta A, Somà A (2004) Modeling and prediction of the dynamic behaviour of microbeams under electrostatic load. *Analog Integr Circuits Signal Process* 40(2):155–164
- Brusa E, De Pasquale G, Somà A (2010b) Characterization of thermo-mechanical coupling in gold microbridges. In: *Proceedings of IEEE DTIP 2010*, 5–7 May 2010, Sevilla, Spain, pp 344–34
- Collard S M (1991) High temperature elastic constants of Gold single-crystals, Dissertation, Rice University, n.9136015, Houston, Texas
- Collenz A, De Bona F, Gugliotta A, Somà A (2004) Large deflections of microbeams under electrostatic loads. *J Micromech Microeng* 14:365–373
- Epp J, Surm H, Hirsch T, Hoffmann F (2011) Residual stress relaxation during heating of bearing rings produced in two different manufacturing chains. *J Mater Process Technol* 211:637–643
- Espinosa HD, Zhu Y, Moldovan N (2006) MEMS-based material testing systems in “encyclopedia of materials: science and technology”. Elsevier, New York
- Goldsmith CL, Forehand DI (2005) Temperature variation of actuation voltage in capacitive MEMS switches. *IEEE Microwirel Compon Lett* 15(10):718–720
- Gupta RK, Gunda JB, Ranga JG, Venkateswara R (2008) Thermal post-buckling analysis of slender columns using the concept of coupled displacement field. *Int J Mech Sci* 52:590–594
- Hasiang Pan C (2002) A simple method for determining linear thermal expansion coefficients of thin films. *J Micromech Microeng* 12:548–555
- Jensen B D, Saitou K, Volakis J L and Kurabayashi K (2003) Fully integrated electrothermal multidomain modeling of RF MEMS switches, *IEEE Microwave and wireless components letters*, 13(9)
- Jing Q (2003) Modeling and simulation for design of suspended MEMS, Ph.D. thesis, Carnegie Mellon University, Pittsburgh, Pennsylvania
- Kang T, Kim JG, Lee JS, Lee JH, Hahn JH, Lee HY, Kim YH (2005) Low-thermal-budget and selective relaxation of stress gradients in gold micro-cantilever beams using ion implantation. *J Micromech Microeng* 15:2469–2478
- Lin L, Chiao M (2000) Self-buckling of micromachined beams under resistive heating. *J MEMS* 9(1):146–151
- Mahameed R, Rebeiz G (2010) A high-power temperature-stable electrostatic RF MEMS capacitive switch based on a thermal buckle-beam design. *J MEMS* 19(4):816–826
- Margesin B, Bagolini A, Guarnieri V, Giacomozzi F, Faes A (2003) Stress characterization of electroplated gold layers for low temperature surface micromachining In: *Proceedings of IEEE/DTIP 2003*, Mandelieu-La Napoule, France, May 2003
- Medvedeva A, Bergström J, Gunnarsson S, Krakhmalev P (2011) Thermally activated relaxation behaviour of shot-peened tool steels for cutting tool body applications. *Mater Sci Eng A* 528:1773–1779
- Motro R (2010) *Anthology of structural morphology*. World Scientific, Singapore
- Mulloni V, Giacomozzi F, Margesin B (2010) Controlling stress and stress gradient during the release process in gold suspended micro-structures. *Sens Actuators A* 162:93–99
- Niemenen H, Ermolov V, Silanto S, Nybergh K, Ryhänen T (2004) Design of a temperature-stable RF MEM capacitor. *J MEMS* 13(5):705–714
- Palego C, Deng J, Peng Z, Halder S, Hwang J, Forehand DI, Scarbrough D, Goldsmith CL, Johnston I, Sampath SI, Datta A (2009) Robustness of RF MEMS Capacitive Switches With Molybdenum Membranes. *IEEE Trans Microw Theory Tech* 57(12):3262–3269
- Rebeiz G (2002) *RF MEMS: theory, design, and technology*, Wiley Interscience, New York
- Reid JR, Starman LA, Webster RT (2003) RF Actuation of Capacitive MEMS Switches. *IEEE MTT-S Digest*, paper TH2D-2

- Rezvani O, Brown C, Zikry MA, Kingon AI, Krim J, Irving DL, Brenner D (2008) The role of creep in the time-dependent resistance of Ohmic gold contacts in radio frequency microelectromechanical system devices. *J Applied Physics* 104(2):024513:1–024513:5
- Rocha LA, Cretu E, Wolffenbuttel RF (2003) Stability of a micromechanical pull-in voltage reference. *IEEE Trans, Inst Meas* 52
- Sadek K, Lueke J, Moussa W (2009) A coupled field multiphysics modeling approach to investigate RF MEMS switch failure modes under various operational conditions. *Sensors* 9:7988–8006
- Saeedivahdat A, Abdolkarimzadeh F, Feyzi A, Rezazadeh G, Tarverdilo S (2010) Effect of thermal stresses on stability and frequency response of a capacitive microphone. *Microelectron J* 41:865–873
- Shamshirsaz M, Asgari MB (2008) Polysilicon microbeams buckling with temperature-dependent properties. *Microsyst Technol* 14:957–961
- Somà A, De Pasquale G (2009) MEMS mechanical fatigue: experimental results on gold microbeams. *J MEMS Trans ASME/IEEE* 18:828–835
- Somà A, De Pasquale G, Brusa E (2010) Effect of residual stress on the mechanical behaviour of microswitches at pull-in threshold. *Strain* 46(4):358–373
- Subhadeep K, Bagolini A, Margesin B, Zen M (2006) Stress and resistivity analysis of electrodeposited gold films for MEMS application. *J Microelectron* 37(11):1329–1334
- Szabo P, Nemeth B, Rencz M (2009) Thermal transient characterisation of the etching quality of micro electro mechanical systems. *Microelectron J* 40:1042–1047
- Tabata O, Tsuchiya T, Brand O, Fedder GK, Hierold C, Korvink JG (2008) Reliability of MEMS: testing of materials and devices, Wiley, Hoboken
- Timoshenko S, Gere J (1961) Theory of elastic stability. McGraw Hill, Tokyo
- Veijola T et al (2009) Experimental validation of compact damping models of perforated MEMS devices. *Microsyst Technol* 15(2):1121–1128
- Yan X (2009) Anelastic stress relaxation in gold films and its impact on restoring forces in MEMS devices. *J MEMS* 18(3):570–576
- Yan D, Yan X, Brown WL, Li Y, Papapolymerou J, Palego C, Hwang JCM, Vinci RP (2004) Design and modeling of a MEMS bidirectional vertical thermal actuator, *J. Micromech Microeng* 14:841–850
- Zamanian M, Khadem SE (2010) Analysis of thermoelastic damping in microresonators by considering the stretching effect. *Int J Mech Sci* 52:1366–1375
- Zhu Y, Espinosa HD (2004) Effect of temperature on capacitive RF MEMS switch performance a coupled-field analysis. *J Micro-mech Microeng* 14:1270–1279